[3]Magnus, W., and Winkler, S., *Hill's Equation*, Interscience, New York, 1966.
[4]Clohessy, W. H., and Wiltshire, R. S., "Terminal Guidance System for Satellite Rendezvous," *Journal of the Aerospace Sciences*, Vol. 27, No. 9, 1960, pp. 653–658.
[5]Alfriend, K. T., Schaub, H., and Gim, D.-W., "Gravitational Perturbations, Nonlinearity and Circular Orbit Assumption Effects on Formation Flying Control Strategies," American Astronautical Society, Paper AAS 00-012, Jan. 2000.
[6]Vadalli, S. R., Alfriend, K. T., and Vaddi, S. S., "A New Concept for Constellation Control of Formation Flying Satellites," American Astronautical Society, Paper AAS 01-218, Feb. 2001.
[7]Gim, D.-W., and Alfriend, K. T., "The State Transition Matrix of Relative Motion for the Perturbed Non-Circular Reference Orbit," American Astronautical Society, Paper AAS 01-222, Feb. 2001.
[8]Melton, R. G., "Time-Explicit Representation of Relative Motion Between Elliptical Orbits," *Journal of Guidance, Control, and Dynamics*, Vol. 23, No. 4, 2000, pp. 604–610.
[9]Kane, T. R., Likins, P. W., and Levinson, D. A., *Spacecraft Dynamics*, McGraw–Hill, New York, 1983, p. 213.
[10]Char, B. W., Geddes, K.O., Gonnet, G. H., Leong, B. L., Monagan, M. B., and Watt, S. M., *First Leaves: A Tutorial Introduction to Maple V*, Springer-Verlag, New York, 1992.

Spacecraft Vibration Reduction Following Thruster Firing for Orbit Adjustment

Arun Banerjee* and Benjamin Diedrich†
Lockheed Martin Missiles and Space Company, Sunnyvale, California 94089

Introduction

WAITING for the decay of vibrations caused by thruster firing reduces time for data taking in spacecraft operations. This Note is concerned with vibration reduction following thruster firing for orbit adjustment. The principle used for vibration reduction in a robust manner is input shaping,[1] which was originally proposed for command shaping in distinct steps and was demonstrated during the shuttle manipulator arm slewing. An equivalent technique implemented in terms of time-delay control was established in Ref. 2. The method of Ref. 1 was extended to constant magnitude on–off thrusters in Ref. 3. Input shaping is an effective and easy-to-implement technique that has been used in disk drive positioning,[4] flexible robot arm control,[5] and many other applications and has been proposed as a baseline design feature for slewing and momentum dumping of the Next Generation Space Telescope.[6]

In this Note we describe two ways of shaping of a thrust–time profile for vibration suppression. The first method uses constant magnitude on–off thrust, where the thruster switching times are computed by solving the input shaping equations of Ref. 1 together with the equation for thrust impulse to be imparted. The second approach uses a two-level thrust by convolution of the thrust pulse with the three-impulse sequence of Ref. 1, and then scales up the torque by the method of Ref. 7. In both cases, input shaping is done for one dominant mode that is excited by the closed-loop control. A detailed nonlinear flexible multibody dynamics model with many appendage vibration modes is then used for simulation of the spacecraft, based on a code with the dynamics formulation of Ref. 8, to verify the effectiveness of vibration suppression.

Received 13 September 2002; revision received 14 March 2003; accepted for publication 21 March 2003.

*Consulting Scientist, Advanced Technology Center, Palo Alto. Associate Fellow AIAA.
†Control Systems Engineer, L1-20/150. Member AIAA.

Table 1 Timed impulse sequence for constant magnitude on off thrust

t_i	A_i
0	1
t_1	−1
t_2	1
t_3	−1
——	——
t_{n-1}	1
t_n	−1

Vibration Reduction Following Thruster Firing

On–off thrust of constant magnitude can be seen as the result of a convolution of a step with the sequence of impulses given in Table 1.

Singer and Seering[1] derived the basic result of robust vibration suppression by applying a sequence of n impulses on a vibratory system. For the timed sequence of impulses of Table 1, the equations for zero residual vibration for the jth mode become

$$\sum_{i=1}^{n}(-1)^i \sin\omega_j t_i = 0, \qquad j = 1, 2, \ldots \tag{1}$$

$$1 + \sum_{i=1}^{n}(-1)^i \cos\omega_j t_i = 0, \qquad j = 1, 2, \ldots \tag{2}$$

Robustness to frequency modeling error gives rise to the equations

$$\sum_{i=1}^{n}(-1)^i t_i \sin\omega_j t_i = 0, \qquad j = 1, 2, \ldots \tag{3}$$

$$\sum_{i=1}^{n}(-1)^i t_i \cos\omega_j t_i = 0, \qquad j = 1, 2, \ldots \tag{4}$$

The requirement of net impulse I for orbit adjustment from thrust of magnitude F translates to the condition

$$F(t_1 + t_3 - t_2 + \cdots + t_n - t_{n-1}) = I \tag{5}$$

For a single mode to suppress, Eqs. (1–5) have five unknown times to solve for three pulses starting at $t = 0$. For two modes to suppress, these represent nine equations in nine unknown times, the solution of which provides five pulses. In general, we see that there is an exact solution possible for the $4n + 1$ impulse times suppressing n modes and meeting the net impulse requirement by $(2n + 1)$ timed pulses.

An alternative to the preceding approach is the scaled convolution method, which scales and successively convolves the thrust–time history with the three-impulse sequence[1] for each vibration mode of period T_i, $i = 1, \ldots, n$:

$$\begin{aligned} F(t) = {} & \alpha F[u(t) - u(t-\tau)] * [0.25\delta(t) + 0.5\delta(t - T_1/2) \\ & + 0.25\delta(t - T_1)] * \cdots * [0.25\delta(t) + 0.5\delta(t - T_n/2) \\ & + 0.25\delta(t - T_n)] \end{aligned} \tag{6}$$

where F is the maximum thruster force; $u(t)$ is the unit step function; $u(t-\tau)$ is the delayed step function, where τ is the unshaped thruster duration; $\delta(t)$ is the impulse function; and $\delta(t - T_i)$ is the impulse function delayed by T_i, the period of vibration of the ith mode to be suppressed. In Eq. (6), α is a scale factor; normally, if the unshaped thruster pulse duration is greater than the period of vibration, α is unity. However, if the nominal thruster firing time is less than the period of vibration, the maximum value of the convolved thrust is less than the available maximum. In such a case, the maximum available thrust is imagined to be scaled up by α so that after convolution the maximum thrust required becomes equal to the real limit. When there are n modes to be suppressed, the right-hand side in Eq. (6) results in a multilevel thrust–time history. This solution reduces to a two-level thrust for a single mode of vibration to suppress.

Numerical Simulation

For numerical demonstration, we consider a spacecraft orbit adjustment that calls for a certain thrust–time impulse to be imparted. A detailed multibody dynamics model that includes the coupled rotational dynamics of the spacecraft with the flexible body dynamics of the solar panels and the dynamics of the controller is used for simulation. Attitude is controlled by a proportional–integral–derivative (PID) controller and the frequency of vibration dominantly excited is estimated from a closed-loop time response for the operating control gain. For a specified impulse requirement for in-track orbit adjustment and the estimated frequency of vibration to suppress, Eqs. (1–5) are solved for the thruster switching times. In all of the simulations to be reported, the thrusters are turned on after 5 s to show the quiescent state maintained by the PID control before thruster firing. Figure 1 shows the results of appendage vibration response with closed-loop control, for in-track tip displacement in response to 3-lbf · s (13.34-N · sec) impulse for scaled covolution (SC), nonlinear equation (NL), and unshaped cases. The three curves in this plot show the superiority of thruster shaping over no shaping and demonstrate the equivalence of the constant magnitude thrust shaping and the stepped thrust given by scaled convolution.

Figure 2 shows the on–off thrust profiles of 3-lbf · s impulse of the constant magnitude shaped and unshaped thruster used in generating

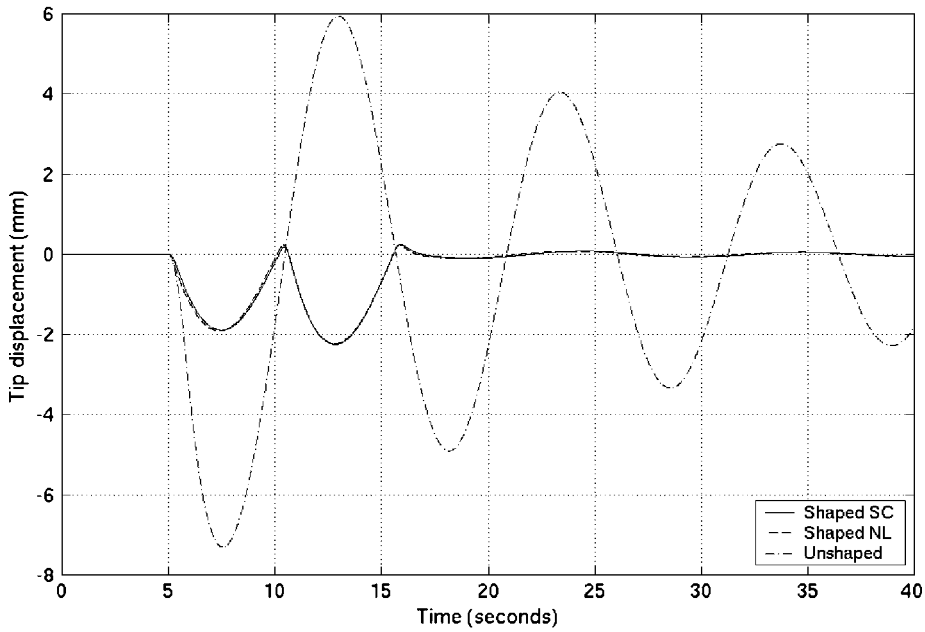

Fig. 1 Vibration response with and without shaping of thruster on–off profile by constant magnitude thrust and stepped thrust due to scaled convolution.

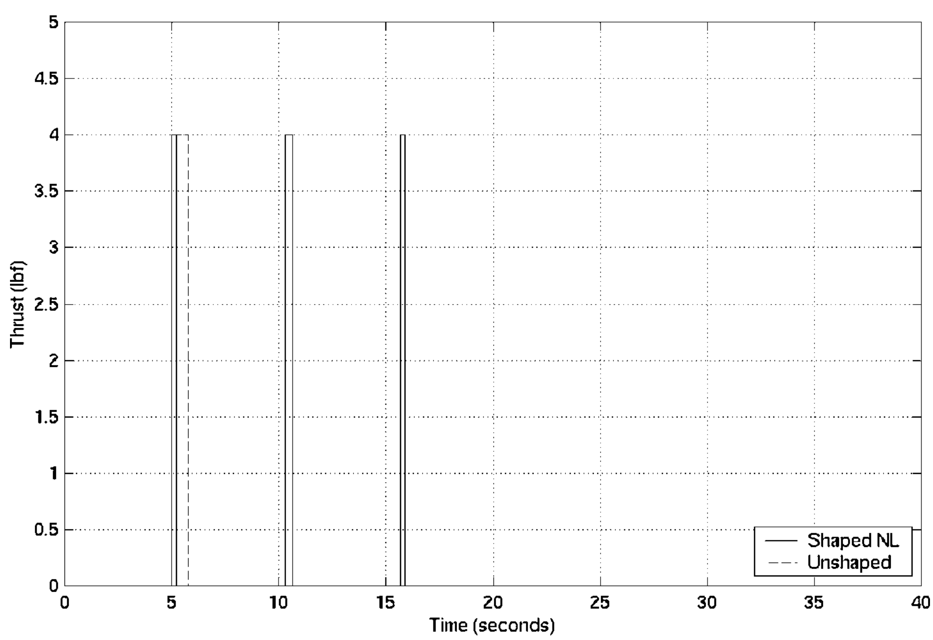

Fig. 2 Thruster on–off profile with and without constant magnitude shaping.

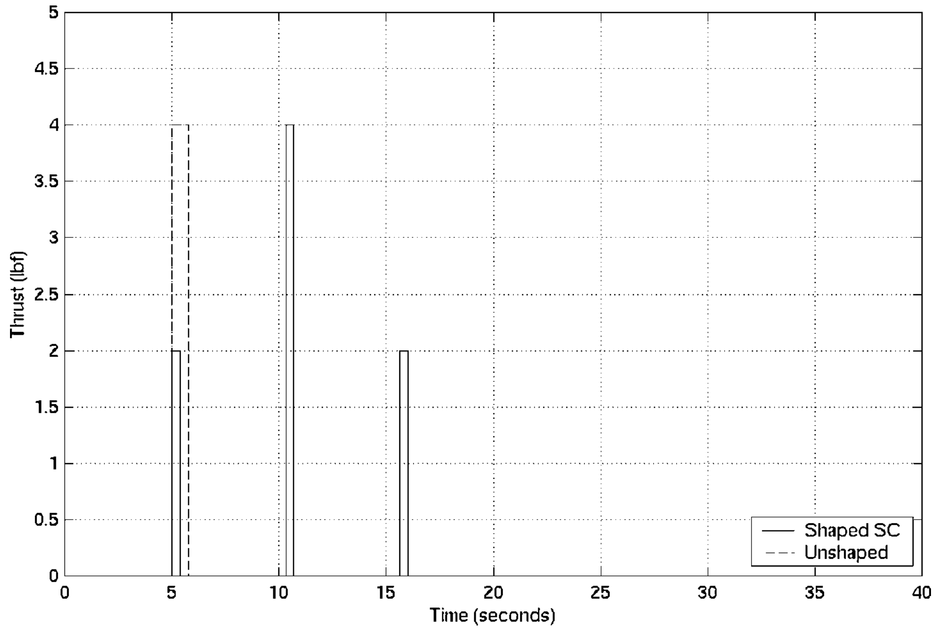

Fig. 3 Thruster on–off profile with and without scaled convolution of thrusters.

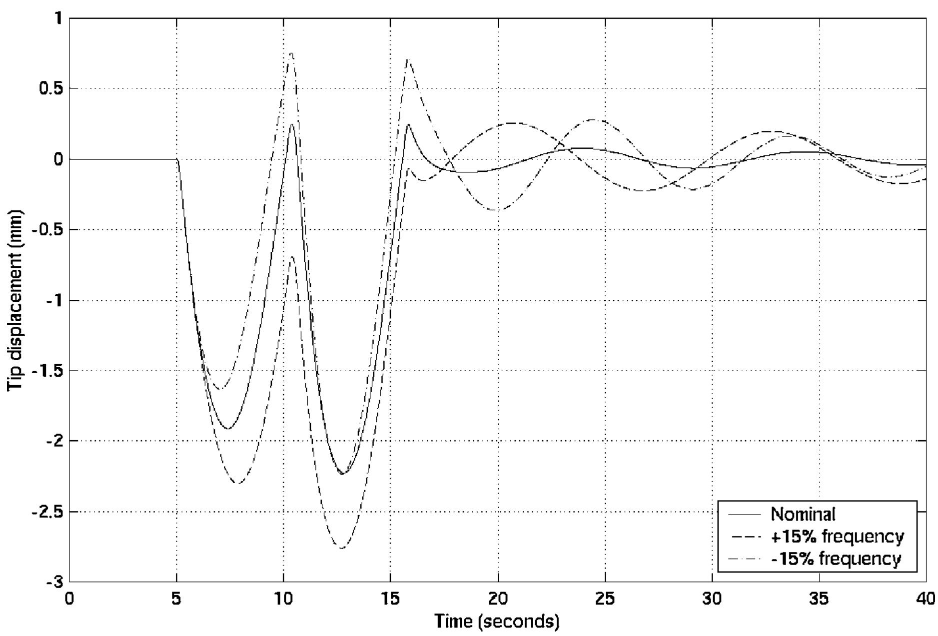

Fig. 4 Demonstration of robustness to knowledge error in shaper frequency.

two of the curves of Fig. 1. Figure 3 shows the thrust profile of 3-lbf · s impulse obtained by SC, compared to the unshaped thrust. Robustness of the thrust shaping solution based on the three-impulse sequence is well known. For the constant magnitude thrust shaping, robustness to knowledge error in frequency of vibration to be suppressed is demonstrated in Fig. 4, by using the nominal on–off thrust–time history for cases when the system frequency is increased and decreased by 15%. From Figs. 1–4, it is clear that the thrust shaping methods are not only effective for vibration reduction but also robust to errors in estimating the frequency of vibration to suppress.

Conclusions

Two equivalent methods for thruster shaping for vibration suppression are presented. The advantage of the first method is that it uses constant magnitude thrust, with the disadvantage that it requires the solution of $4n + 1$ nonlinear equations for suppressing n modes of vibration. The second method has the advantage of simpler computation, being based on direct convolution with scaling of the three-impulse sequence for a mode, but has the disadvantage of a multiple-step-level thrust. It is shown that input shaping of thrusters is quite effective and robust to frequency errors in reducing vibrations following thruster firing. Any desired change in tuning frequency can be recognized from attitude control gyro data from the spacecraft. The method does not require frequent firing of thrusters and comfortably meets usual minimum-pulse-width margins. Thruster misalignment may cause attitude errors but will not affect vibration reduction if the switching times are maintained; thruster uncertainty in achieving desired on–off times will, however, adversely affect vibration suppression beyond the robustness threshold.

References

[1]Singer, N. C., and Seering, W. P., "Preshaping Command Inputs to Reduce System Vibration," *Journal of Dynamic Systems, Measurement, and Control*, Vol. 112, March 1990, pp. 76–82.

[2]Singh, T., and Vadali, S. R., "Robust Time-Delay Control," *Journal of Dynamic Systems, Measurement, and Control*, Vol. 115, March 1993, pp. 303–306.

[3]Singhose, W., Banerjee, A. K., and Seering, W. E., "Slewing Flexible Spacecraft with Deflection Limiting Input Shaping," *Journal of Guidance, Control, and Dynamics*, Vol. 20, No. 2, 1997, pp. 291–298.

[4]Cutforth, C. F., and Pao, L. Y., "Command Shaping Controller for Vibration Reduction without Lengthening the Command," AIAA Paper 2000-3956, Aug. 2000.

[5]Marcello, R., Agrawal, B. N., and Bernelli-Zazzera, F., "Experiments on Command Shaping Control of a Manipulator with Flexible Links," *Journal of Guidance, Control, and Dynamics*, Vol. 25, No. 2, 2002, pp. 232–239.

[6]Banerjee, A. K., Pedreiro, N., and Singhose, W., "Vibration Reduction for Flexible Spacecraft Following Momentum Dumping with/without Slewing," *Journal of Guidance, Control, and Dynamics*, Vol. 24, No. 3, 2001, pp. 417–428.

[7]Banerjee, A. K., "Reducing Minimum Time for Small Angle Slewing of a Flexible Body," *Journal of Guidance, Control, and Dynamics*, Vol. 24, No. 5, 2001, pp. 1040–1043.

[8]Banerjee, A. K., "Block-Diagonal Equations for Flexible Multibody Dynamics with Geometric Stiffness and Constraints," *Journal of Guidance, Control, and Dynamics*, Vol. 16, No. 6, 1993, pp. 1092–1100.

Azimuthal Repositioning of Payloads in Heliocentric Orbit Using Solar Sails

Colin R. McInnes*

University of Glasgow, Glasgow, Scotland G12 8QQ, United Kingdom

I. Introduction

FUTURE solar physics missions will require the ability to reposition multiple spacecraft at different azimuthal positions relative to the Earth, while remaining close to a one year circular orbit. Such azimuthal repositioning will allow stereoscopic views of solar features to be generated and will allow imaging of coronal mass ejections as they transit the sun–Earth line. The NASA STEREO mission, which is scheduled for launch in 2005, will utilize two spacecraft to perform such tasks. Both spacecraft will be launched on a Delta II 7925 and will use multiple lunar gravity assists to maneuver the spacecraft onto leading and trailing heliocentric orbits. The two spacecraft will then drift ahead of and behind the Earth on free-drift trajectories, with increasing Earth–sun–spacecraft angles.

One limitation of such free-drift trajectories is that the Earth–sun–spacecraft angle is uncontrolled. It would be advantageous to stop the spacecraft drift at certain azimuthal positions relative to the Earth to perform various observing campaigns. Different observations require different spacecraft angular separations to optimize the mission science return. In principle, such control is possible by using chemical propulsion to start and stop the azimuthal drift. However, as will be seen, such maneuvers can incur a large accumulated Δv. In this Note, the use of small solar sails is investigated to control the spacecraft azimuthal drift using solar radiation pressure. Because propellant mass is not an issue for solar sails, there are benefits in launch mass reduction over chemical propulsion.

The problem is investigated using analytical methods by linearizing the solar sail two-body equations of motion in the vicinity of the Earth's orbit. When polar coordinates are used, only small departures in orbit radius are required to ensure that the linear solutions provide a good representation of the solar sail trajectory. A simple two-step sail steering strategy is then investigated and the sail attitude is optimized to provide the largest change in azimuthal position relative to the Earth for a fixed maneuver duration. Last, a comparison is made with chemical propulsion, and the benefits of solar sail propulsion for such maneuvers is assessed.

II. Relative Equations of Motion

The heliocentric equations of motion for an ideal, planar solar sail may be written in plane polar coordinates (r, θ) as[1]

$$\ddot{r}(t) - r(t)\dot{\theta}(t)^2 = -[\mu/r(t)^2](1 - \beta\cos^3\alpha) \tag{1a}$$

$$r(t)\ddot{\theta}(t) + 2\dot{r}(t)\dot{\theta}(t) = \beta[\mu/r(t)^2]\cos^2\alpha\sin\alpha \tag{1b}$$

where $r(t)$ is the heliocentric distance of the solar sail from the sun at time t, $\theta(t)$ is the polar angle of the solar sail measured from some reference direction, and μ is the gravitational parameter of the problem. Because both solar radiation pressure and solar gravity have an inverse square variation with heliocentric distance, the sail performance can be parameterized by the sail lightness number β, defined as the ratio of the solar radiation force to the solar gravitational force acting on the solar sail. The total sail mass per unit area σ is related to β using $\beta = 1.53/\sigma$ $(g \cdot m^{-2})$ (Ref. 1). The sail pitch angle α is defined as the angle between the sun–sail line and the sail normal.

Here, we are interested in trajectories that will result in a large change in polar angle, but only a small change in orbit radius. In orbit to investigate such trajectories analytically, a new set of coordinates will be defined to facilitate the linearization of Eqs. (1), as shown in Fig. 1. The coordinates will be referenced to the instantaneous position of the Earth, given in polar coordinates (r, θ) by $[R, \omega(t - t_0)]$, where R is the orbit radius of the Earth and $\omega = \sqrt{(\mu/R^3)}$ is the orbital angular velocity of the Earth. When defining $\xi(t) = r(t) - R$ and $\phi(t) = \theta(t) - \omega(t - t_0)$, the equations of motion can be linearized to allow analysis using analytical methods.

Equations (1) will now be expanded to first order, so that terms of order $(\xi/R)^2$ and above are neglected. In addition, because only small solar sails will be considered, terms of order $\beta(\xi/R)$ are taken as second order and so are neglected. Neglecting these mixed terms

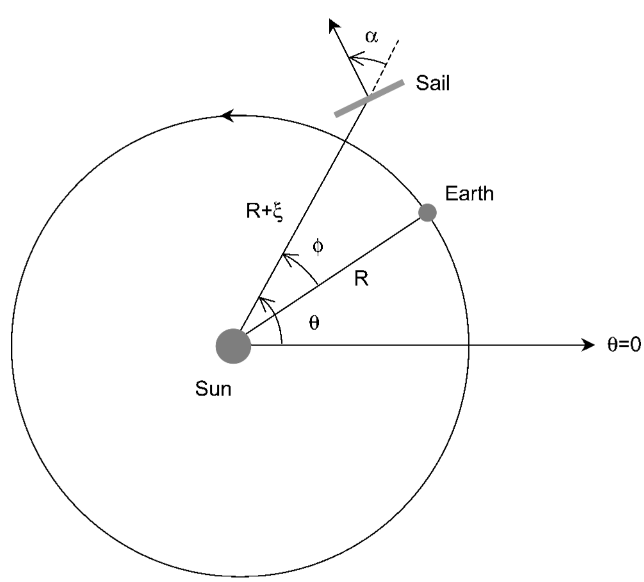

Fig. 1 Solar sail polar coordinates transformed relative to the Earth.

Received 10 March 2003; revision received 21 March 2003; accepted for publication 21 March 2003.

*Professor, Department of Aerospace Engineering; colinmc@aero.gla.ac.uk.